

Differential Effects of Teriparatide on Regional Bone Formation Using ^{18}F -Fluoride Positron Emission Tomography

Michelle L Frost,¹ Musib Siddique,¹ Glen M Blake,¹ Amelia EB Moore,¹ Paul J Schleyer,² Joel T Dunn,² Edward J Somer,² Paul K Marsden,² Richard Eastell,³ and Ignac Fogelman¹

¹Osteoporosis Research Unit, Division of Imaging Sciences, King's College London, Guy's Campus, London, UK

²Clinical PET Centre, Division of Imaging Sciences, King's College London, St Thomas' Campus, London, UK

³Academic Unit of Bone Metabolism, University of Sheffield, Sheffield, UK

ABSTRACT

Teriparatide increases skeletal mass, bone turnover markers, and bone strength, but local effects on bone tissue may vary between skeletal sites. We used positron emission tomography (PET) to study ^{18}F -fluoride plasma clearance (K_i) at the spine and standardized uptake values (SUVs) at the spine, pelvis, total hip, and femoral shaft in 18 postmenopausal women with osteoporosis. Subjects underwent a 1-hour dynamic scan of the lumbar spine and a 10-minute static scan of the pelvis and femurs at baseline and after 6 months of treatment with 20 $\mu\text{g}/\text{day}$ teriparatide. Blood samples were taken to derive the arterial input function and lumbar spine K_i values evaluated using a three-compartment model. SUVs were calculated for the spine, pelvis, total hip, and femoral shaft. After 6 months treatment with teriparatide, spine K_i values increased by 24% ($p = .0003$), while other model parameters were unchanged except for the fraction of tracer going to bone mineral ($k_3/[k_2 + k_3]$), which increased by 23% ($p = .0006$). In contrast to K_i , spine SUVs increased by only 3% ($p = .84$). The discrepancy between changes in K_i and SUVs was explained by a 20% decrease in ^{18}F plasma concentration. SUVs increased by 37% at the femoral shaft ($p = .0019$), 20% at the total hip ($p = .032$), and 11% at the pelvis ($p = .070$). Changes in bone turnover markers and BMD were consistent with previous trials. We conclude that the changes in bone formation rate during teriparatide treatment as measured by ^{18}F PET differ at different skeletal sites, with larger increases in cortical bone than at trabecular sites. © 2011 American Society for Bone and Mineral Research.

KEY WORDS: TERIPARATIDE; BONE FORMATION; OSTEOPOROSIS; POSITRON EMISSION TOMOGRAPHY; ^{18}F -FLUORIDE

Introduction

The last 20 years have seen the development of a series of increasingly potent new treatments for the prevention of osteoporotic fractures.^(1–8) Generally, these can be divided into two types: (1) antiresorptive treatments such as bisphosphonates^(1,2,4,6,7) that bring about a prompt decrease in biochemical markers of bone resorption followed a few months later by a reduction in bone formation markers⁽⁹⁾ and (2) anabolic agents (currently only parathyroid hormone)^(5,10) that bring about a prompt increase in bone formation followed a few weeks later by an increase in bone resorption.⁽¹¹⁾

Many modern treatments for osteoporosis have a profound effect on bone remodeling, and studies of bone turnover have an important role in the evaluation of their effect on bone quality.^(12–16) Bone biopsy with double tetracycline labelling is

considered the gold standard for the direct assessment of bone turnover activity, but it is complex, invasive, and costly, and restricted to a single site, the iliac crest.^(13–16) The most commonly used and practical method is the measurement of bone turnover markers (BTMs) in serum and urine, which have the advantage of a large and rapid response seen in patients commencing treatment for osteoporosis.^(9,11)

Because BTMs provide information on the integrated response across the whole skeleton, they cannot provide insight into the changes that occur at specific sites such as the spine or hip or differentiate between the responses in trabecular and cortical bone. Radionuclide imaging provides a novel method of studying regional bone metabolism.⁽¹⁷⁾ One of the most widely used techniques is ^{18}F -fluoride positron emission tomography (^{18}F PET) analyzed using the method described by Hawkins et al.^(18–23) In the Hawkins method, the bone time-activity curve

Received in original form August 25, 2010; revised form October 31, 2010; accepted November 18, 2010. Published online December 2, 2010.

Address correspondence to: Glen M Blake, Osteoporosis Research Unit, 1st Floor, Tower Wing, Guy's Hospital, London, SE1 9RT, United Kingdom
E-mail: glen.blake@kcl.ac.uk

Journal of Bone and Mineral Research, Vol. 26, No. 5, May 2011, pp 1002–1011

DOI: 10.1002/jbmr.305

© 2011 American Society for Bone and Mineral Research

and the arterial tracer input function are analyzed using a three-compartment model to derive the regional bone plasma clearance (K_p ; units $\text{mL min}^{-1} \text{mL}^{-1}$).

Bone plasma clearance quantifies the rate of $^{18}\text{F}^-$ uptake into bone tissue in terms of its concentration in plasma, providing a measurement that is responsive to changes in bone blood flow and osteoblastic activity.⁽¹⁷⁾ Plasma clearance is widely used to study organ function, such as the use of glomerular filtration rate (defined as the renal plasma clearance of inulin) to measure kidney function. The use of bone plasma clearance measured using $^{18}\text{F}^-$ PET to study bone formation was validated in two reports that found high correlations between the bone kinetic parameters obtained using $^{18}\text{F}^-$ PET and histomorphometric indices of bone formation and mineral apposition rate.^(24,25) A simpler method of quantifying radionuclide studies that avoids the need to take blood samples to find the plasma concentration is to measure the uptake in the organ being studied. An example is the gamma camera method of measuring the skeletal uptake of $^{99\text{m}}\text{Tc}$ -methylene diphosphonate ($^{99\text{m}}\text{Tc}$ -MDP) described by Brenner et al.⁽²⁶⁾ For $^{18}\text{F}^-$ PET studies, an equivalent measurement of bone uptake is provided by standardized uptake values (SUVs), which normalize the concentration in the bone region of interest for injected activity and body weight ($\text{SUV} = \text{mean kBq/mL} \times \text{body weight [kg]} / \text{injected activity [MBq]}$).⁽²⁷⁾

The only previous studies that used $^{18}\text{F}^-$ PET to examine the regional effects of an osteoporosis treatment were a report by Frost et al.⁽²¹⁾ on the effect of risedronate on bone turnover at the lumbar spine and a study by Uchida et al.⁽²⁷⁾ on the effects of alendronate on bone metabolism at the spine and femoral neck in glucocorticoid-induced osteoporosis. To date, no studies of an anabolic agent have been reported. Recombinant parathyroid hormone fragment rhPTH(1-34) (teriparatide) is an anabolic therapy approved for use in women and men with osteoporosis at high risk for fracture^(5,28) that preferentially stimulates osteoblast over osteoclast activity, resulting in new bone formation and large increases in the rate of bone remodeling as measured by BTMs and bone histomorphometry.⁽¹¹⁻¹⁶⁾

In this study, $^{18}\text{F}^-$ PET imaging was used to assess the impact of teriparatide on regional bone metabolic response at the lumbar spine, pelvis, and proximal femur. The primary aims of the study were to evaluate the effect of 20 $\mu\text{g}/\text{day}$ teriparatide on $^{18}\text{F}^-$ plasma clearance at the lumbar spine in postmenopausal women with osteoporosis and compare the effects of teriparatide treatment on SUVs at the spine, pelvis, hip, and femoral shaft. Additional aims were to examine the correlations between changes in $^{18}\text{F}^-$ plasma clearance with changes in BTMs and BMD changes at the spine and hip.

Materials and Methods

Subjects

We recruited 20 postmenopausal women (mean age 65 years, range 52–77) who had a BMD T -score of -2.5 or less at the spine or hip and had osteoporosis as defined by World Health Organization (WHO) criteria.⁽²⁹⁾ None of the women had previously received any treatment for osteoporosis, and none had any other disease that affected bone metabolism. Routine

laboratory tests of serum calcium, albumin-corrected calcium, alkaline phosphatase (ALP), phosphate, parathyroid hormone (PTH) and 25-hydroxy vitamin D were performed at baseline, and all except PTH and vitamin D were repeated at 1-, 3- and 6-month follow-up visits. Dynamic $^{18}\text{F}^-$ PET scans of the lumbar spine followed by static scans of the pelvis and both upper femurs were performed at baseline and at 6 months. Subjects commenced treatment with 20 $\mu\text{g}/\text{day}$ teriparatide by subcutaneous self-injection starting the day after their first PET scan and continued for 6 months. The women also received daily calcium (600–1200 mg) and vitamin D (400–800 IU) for the duration of the study. Compliance with teriparatide treatment was assessed by measuring the residual volume in the injection pens. Informed written consent was obtained from all participants and the local Research Ethics Committee approved the study.

Measurements of BMD and biochemical markers of bone turnover

Dual-energy X-ray absorptiometry (DXA) BMD measurements at the lumbar spine (L1–L4), femoral neck, and total hip were performed using a Hologic Discovery (Hologic, Bedford, MA, USA) at the baseline and 6-month visits. The long-term precision was 1.6% for spine, 2.5% for femoral neck, and 1.6% for total hip BMD.⁽³⁰⁾

Blood and urine samples for BTM measurements were taken at baseline, 1 month, 3 months, and 6 months and were collected at the same time of day at each visit. Serum bone-specific alkaline phosphatase (bone ALP) and serum procollagen propeptide of type 1 collagen (PINP) were measured as markers of bone formation. Serum cross-linked C-telopeptide of type-I collagen (sCTX) and fasting measurements of urinary cross-linked N-telopeptide of type-I collagen normalized to creatinine (uNTX/Cr) were used as markers of bone resorption. Bone ALP was measured by paramagnetic particle immunoassay (Access 2, Beckman Coulter, Brea, CA, USA) with an interassay coefficient of variation (CV) of 5.2%. PINP was measured by electrochemiluminescent immunoassay (Roche Elecsys, Roche Diagnostics, Basel, Switzerland; interassay CV: 3.7%). sCTX was measured by electrochemiluminescent immunoassay (Roche Elecsys, Roche Diagnostics), with an interassay CV of 4.0%. uNTX was expressed as a ratio to urinary creatinine (uCr), which was measured by dry-slide chemistry (Vitros 250, OrthoDiagnostics, Rochester, NY, USA; interassay CV: 5.9%). Samples were stored at -70°C and all samples collected from each individual subject were analyzed in the same batch.

PET image acquisition and analysis

The PET studies were acquired on a GE Discovery PET/CT scanner (General Electric Medical Systems, Waukesha, WI, USA) with a 15-cm axial field of view. Subjects were positioned supine with four lumbar vertebrae (L1–L4) in the field of view, and CT images were acquired for attenuation correction. After an intravenous injection of 90 MBq of tracer, a 60-minute dynamic scan consisting of twenty-four 5-second, four 30-second, and fourteen 240-second time frames was begun simultaneously with the bolus injection. At the end of the dynamic scan, two 5-minute

static scans of the pelvis and upper femurs with a total field of view of 30 cm were acquired, starting 65 minutes after injection of tracer and together with CT images for attenuation correction.

All activity measurements were corrected for radioactive decay to the time of injection. Regions of interest (ROI) in the lumbar spine were defined by summing the final twelve 240-second dynamic frames and placing an elliptical ROI within each vertebral body, avoiding the end-plates and disk space, to generate bone time-activity curves (units: kBq/mL). The final lumbar spine time-activity curve for each subject was produced by averaging results for the four individual vertebral bodies. The bone time-activity curve was also normalized for injected activity and the subject's body weight to produce dynamic curves of the mean standardized uptake value (SUV_{mean}) in the bone ROI between 10 and 60 minutes after tracer injection.

The static PET scans of the pelvis and upper femurs were analyzed to obtain values of SUV_{mean} in four ROI: (1) a 60-mm section of cortical bone in the upper femoral shaft measured from just below the lesser trochanter; (2) a region of mixed trabecular and cortical bone between the femoral neck and lesser trochanter anatomically equivalent to the total hip ROI used in DXA scanning;⁽³¹⁾ (3) the whole of the pelvis; and (4) trabecular bone in the fifth lumbar vertebra (L5). SUV figures for L5 were obtained in the same way as those for L1–L4, by placing an elliptical ROI within the vertebral body. SUV figures for the pelvis and proximal femur were obtained by using the CT image to identify the bone and define ROIs for the right- and left-upper femoral shaft, the right and left total hip, and the pelvis, which were then mapped onto the PET image. SUVs were calculated separately for the right and left sides of the proximal femur before averaging.

Arterial plasma input function

To obtain measurements of $^{18}F^-$ skeletal plasma clearance, the arterial input function is required. Venous blood samples were taken at 2, 4, 10, 20, 30, 40, 50, and 60 minutes after tracer injection, whole blood samples were centrifuged, and the plasma concentration of $^{18}F^-$ (units: kBq/mL) measured using a well counter that was cross-calibrated daily with the PET scanner using ^{68}Ge standards. The input function was estimated using a semi-population curve method based on direct arterial sampling in 10 postmenopausal women studied by Cook et al.⁽²⁰⁾ Cook showed that for $^{18}F^-$ the tracer concentrations in arterial and venous blood are equal by 30 minutes after injection. A single exponential was fitted to the 30, 40, 50 and 60-minute venous plasma concentrations to define the terminal exponential for the 0- to 60-minute dynamic scan. Venous data for the 10 women studied by Cook were analyzed in the same way, and the terminal exponential was subtracted from the full arterial curve measured by direct sampling to define the residual curve representing the bolus peak and sum of the early fast exponentials. The residual curves in the 10 women were adjusted so the times of peak activity concentration were coincident and averaged to define the mean population residual curve. For each subject in the present study, the population residual curve was scaled for injected activity and, after adjusting the time of peak count rate to the time determined from an ROI drawn on the

dynamic scan over the aorta, the scaled and time-adjusted population residual was added to the individual's terminal exponential curve to obtain the 0- to 60-minute arterial input function used for kinetic analysis (Fig. 1).

$^{18}F^-$ fluoride kinetic analysis

The data from the PET dynamic spine scan were processed using the three-compartment model described by Hawkins et al. to estimate the $^{18}F^-$ bone plasma clearance to the lumbar vertebral bodies (Fig. 2).⁽¹⁸⁾ In the Hawkins model, the rate constant K_1 describes the plasma clearance of tracer to the bone extravascular (bone ECF) compartment, k_2 the reverse transport of tracer from the bone ECF back to plasma, k_3 the forward transport from bone ECF to the bone mineral compartment, and k_4 the reverse flow. The parameter K_i , representing the plasma clearance to the bone mineral compartment, is calculated from the following equation:

$$K_i = K_1 \times k_3 / (k_2 + k_3) \text{ mL min}^{-1} \text{ mL}^{-1} \quad (1)$$

SUVs provide a model independent method of evaluating $^{18}F^-$ skeletal kinetics.⁽²²⁾ For this purpose, the SUV data for the last 2 time frames of the dynamic study (52–60 minutes) were averaged to calculate the end-of-study spine SUV_{mean} . SUVs at 65–75 minutes for the upper femoral shaft and total hip sites (mean of left and right sides), the pelvis, and L5 were taken from the analysis of the static PET scans.

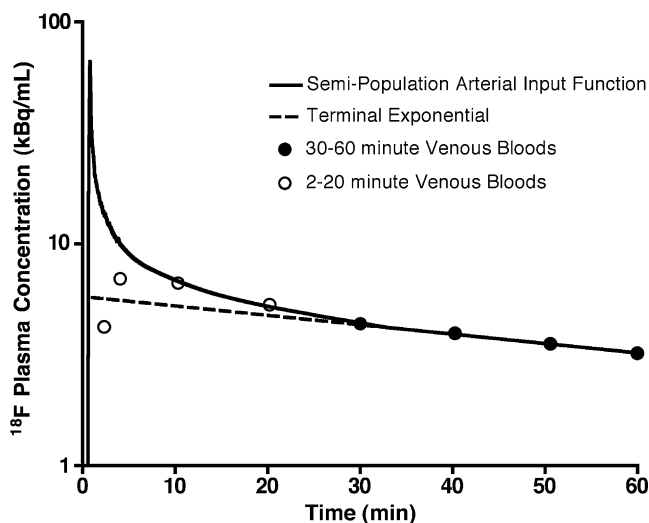


Fig. 1. Derivation of the $^{18}F^-$ arterial plasma input function by a semi-population method after fitting a single exponential to the 30-, 40-, 50-, and 60-minute venous blood measurements in each subject. The full plasma input function is obtained by adding a curve representing the bolus peak and fast exponentials derived from continuous arterial sampling in 10 postmenopausal women studied by Cook et al scaled for injected activity.⁽²⁰⁾ The time of peak concentration was set from the time-activity curve of a region of interest (ROI) drawn over the aorta of the dynamic spine scan. Venous blood points at 2 and 4 minutes lie below the arterial curve because venous and arterial bloods do not reach equilibrium until 30 minutes after injection.

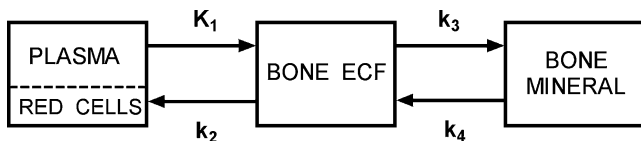


Fig. 2. Three-compartment 4k bone kinetic model described by Hawkins et al. for the analysis of ^{18}F -fluoride PET dynamic bone studies.¹⁸ See text for description of rate constants. Red cells = red blood cells; ECF = extracellular fluid.

Statistical analysis

Baseline characteristics of the study population were expressed as the mean and standard deviation (SD). The changes in BMD and BTMs and measures of ^{18}F skeletal tracer kinetics were expressed as the percentage change from baseline and, after testing for normality, parametric or nonparametric tests were used accordingly. Changes that passed the tests for normality were expressed as the mean and SD and evaluated using the paired Student *t*-test. Otherwise, the changes were expressed by the median and interquartile range (IQR) and evaluated using the Wilcoxon signed rank test. Correlations between changes in the bone kinetic parameters and changes in BMD and BTMs were assessed using the Spearman rank correlation test. Changes in the curves of ^{18}F plasma concentration and lumbar spine SUVs against time between the baseline and 6-month PET scans were assessed using a two-way repeated-measures analysis of variance (ANOVA) test.⁽³²⁾ A *p* value of .05 or less was considered statistically significant.

Results

Study Population

Baseline characteristics of the twenty women who participated in the study are shown in Table 1. The subjects were all postmenopausal, with a mean time since menopause of 17.7 years (range 2 to 33 years). The women all had osteoporosis at the spine and/or hip, with a minimum *T*-score at the spine (L1–L4), femoral neck, or total hip sites between -2.5 and -4.1 . Six out of twenty women (30%) had previously sustained a low-trauma fracture, although these all occurred a minimum of 12 months before the baseline scan and none affected the ^{18}F uptake. Serum calcium, albumin corrected calcium, serum phosphate, alkaline phosphatase, and PTH levels were within normal limits for all subjects. Biochemical markers of bone turnover at baseline were within the range expected for postmenopausal women. Compliance with teriparatide treatment over the 6-month period averaged 96% (range 70 to 104%).

Bone Density Measurements and Biochemical Markers of Bone Turnover

The final follow-up studies were performed 6.0 months (range 5.5 to 6.4 months) after the baseline visit. The mean percentage changes (SD) in BMD at the lumbar spine, femoral neck, and total hip at 6 months were $+5.6$ (5.4) % ($p = .0002$), -1.3 (3.8) % ($p = .13$) and -0.6 (2.4) % ($p = .27$), respectively (Table 2). After 6 months of teriparatide treatment, there were highly statistically significant increases in serum PINP, bone ALP, sCTX, and uNTX/

Table 1. Demographics and Baseline Characteristics ($N = 20$)

Characteristic	Mean \pm SD	Normal Range
Age (years)	65.3 \pm 8.2	----
Years Postmenopausal	17.7 \pm 9.1	----
Body Mass Index (kg/m ²)	24.6 \pm 3.3	----
Number with Prevalent Fractures	6/20 (30%)	----
Lumbar Spine <i>T</i> -score	-3.0 ± 0.7	----
Femoral Neck <i>T</i> -score	-2.0 ± 0.6	----
Serum Calcium (mmol/L)	2.4 \pm 0.1	2.15 – 2.55
Corrected Calcium (mmol/L)	2.4 \pm 0.1	2.15 – 2.55
Serum Phosphate (mmol/L)	1.2 \pm 0.1	0.9 – 1.4
Serum Alkaline Phosphatase (AP) (U/L)	75 \pm 13	35 – 129
Parathyroid Hormone (ng/L)	37 \pm 15	10 – 65
25-Hydroxy Vitamin D (nmol/L)	62 \pm 19	> 60

SD, standard deviation. Normal ranges are from Guy's & St Thomas NHS Trust Clinical Chemistry Department

creatinine ratio (Fig. 3, Table 2). Some of the bone markers also showed statistically significant changes at the 1- and 3-month time points. Concentrations of serum ALP showed median percent changes (IQR) from baseline of $+4.9\%$ (-4.9% – 15.5%) at 1 month ($p = .28$), $+16.1\%$ (2.2% – 19.0%) at 3 months ($p = .022$) and $+28.7\%$ (6.8% – 44.6%) at 6 months ($p = .0009$).

Quantitative Measurements of Bone Metabolism using ^{18}F -Fluoride

Baseline and follow-up ^{18}F PET studies were available for a total of 18 women. Measurements of the ^{18}F plasma clearance to the bone mineral compartment of the lumbar vertebral bodies showed a highly significant change from baseline with a mean percentage increase (SD) of 23.8% (22.4%) ($p = .0003$) (Fig. 4A, Table 2). Mean values of the other kinetic parameters of the three-compartment model before and after teriparatide treatment and their statistical significance are listed in Table 2. Apart from K_i , the only other statistically significant change was in the ratio $k_3/(k_2 + k_3)$, representing the fraction of tracer in the bone ECF compartment going to bone mineral, which increased by 23% from 0.33 to 0.40 ($p = .0006$).

In contrast to the highly significant changes in spine plasma clearance measured by K_i , the changes in bone uptake as measured by the SUVs at the end of the 60-minute dynamic study were not significantly different from zero (Fig. 4B, Table 2). The mean percent change (SD) in SUVs from baseline was $+3.0\%$ (15.9%) ($p = .84$). A plot of the change in ^{18}F plasma concentration from 10 to 60 minutes after injection showed that the 3% change in SUVs was explained by the combined effects of the 24% increase in plasma clearance, with a 20% decrease in ^{18}F plasma concentration (Fig. 5A). The two-way repeated-measures ANOVA of the ^{18}F plasma data showed a highly significant treatment effect ($p = .0004$) with no evidence of an interaction term between treatment and time ($p = .10$) (Fig. 5A). A similar analysis of the 10- to 60-minute SUV curves showed no evidence of any treatment effect ($p = .72$) and no interaction term ($p = .98$) (Fig. 5B).

Table 2. Mean ^{18}F -fluoride Kinetic Parameters, Bone Turnover Markers, and BMD at Baseline and After 6 Months Treatment With Teriparatide

	Baseline mean (SD)	6 months mean (SD)	Mean % change (SD) ^a	<i>p</i> Value ^b
Dynamic spine scan				
K_1 (mL min ⁻¹ mL ⁻¹)	0.035 (0.009)	0.043 (0.010)	+23.8 (22.4) %	.0003
K_1 (mL min ⁻¹ mL ⁻¹)	0.106 (0.013)	0.108 (0.026)	+1.8 (18.9) %	.65
k_2 (min ⁻¹)	0.382 (0.229)	0.357 (0.185)	+8.3 (52.9) %	.63
k_3 (min ⁻¹)	0.177 (0.078)	0.229 (0.093)	+52.5 (81.7) %	.069
k_4 (min ⁻¹)	0.011 (0.004)	0.011 (0.004)	+21.1 (68.2) %	.76
$k_3/(k_2 + k_3)$	0.332 (0.074)	0.403 (0.094)	+23.4 (22.7) %	.0006
SUV _{mean} Spine (L1-L4)	5.66 (1.09)	5.70 (0.79)	+3.0 (15.9) %	.84
Static hip scan				
SUV _{mean} Spine (L5)	6.92 (2.12)	6.80 (2.53)	-1.9 (15.5) %	.69
SUV _{mean} Femoral shaft	2.07 (0.64)	2.77 (1.02)	+36.9 (40.3) %	.0019
SUV _{mean} Total hip	2.49 (0.93)	2.93 (1.22)	+19.8 (27.2) %	.032
SUV _{mean} Pelvis	3.71 (1.14)	4.11 (1.49)	+11.1 (20.7) %	.070
Bone turnover markers				
Bone ALP (ng mL ⁻¹)	10.0 (3.9)	20.2 (12.4)	+76.4% (28.1–152%)	.0009
PINP (ng mL ⁻¹)	44.3 (19.3)	205.0 (138.3)	+258% (130–386%)	.0003
sCTX (ng mL ⁻¹)	0.199 (0.141)	0.581 (0.525)	+218% (85–500%)	.0005
uNTX (nmol BCE/mmol Cr)	70.6 (27.6)	112.0 (72.3)	+35.7% (6.1–123.0%)	.007
DXA BMD				
Spine BMD (g cm ⁻²)	0.716 (0.078)	0.755 (0.080)	+5.6 (5.4) %	.0002
Femoral neck BMD (g cm ⁻²)	0.629 (0.067)	0.621 (0.066)	-1.3 (3.8) %	.13
Total hip BMD (g cm ⁻²)	0.738 (0.068)	0.734 (0.070)	-0.6 (2.4) %	.27

^aResults are mean and SD of the percentage change from baseline for individual subjects except for bone turnover markers which are the median and interquartile range

^b*P* values calculated using a paired *t*-test apart from bone turnover markers, which were calculated using the Wilcoxon signed rank test.

SUVs for L5 measured from the static PET scan confirmed the finding from the dynamic spine scan that there was no significant change in figures for trabecular bone in the vertebral bodies (Table 2). In contrast, SUVs for cortical bone in the femoral shaft increased by 36.9% ($p = .0019$) (Fig. 4C), and these changes were statistically significantly larger than those measured at the lumbar spine on the dynamic scan ($p = .005$). Changes in SUVs in the total hip and pelvis were intermediate between those seen in the femoral shaft and lumbar spine, with average increases of 19.8% for the total hip site ($p = .032$) (Fig. 4D) and 11.1% for the pelvis ($p = .070$) (Table 2).

The Spearman rank correlation coefficients between changes in spine plasma clearance and changes in BTMs after 6 months of teriparatide therapy are shown in Table 3. None of the four correlations were statistically significant, with *p*-values ranging between .34 and .87. In contrast, 4 out of 6 correlations between the changes in PINP, bone BSAP, uNTX, and sCTX were statistically significant ($p < .05$). The Spearman correlation coefficient between the changes in spine plasma clearance and the BMD changes were not significant for the spine ($R = 0.253; p = .31$), femoral neck ($R = -0.238; p = .34$) or total hip sites ($R = -0.364; p = .14$).

Discussion

This study used ^{18}F -PET imaging to evaluate the effects of teriparatide treatment on bone metabolic response and to

examine the changes at a cortical bone site in the femoral shaft and trabecular bone in the spine. Although bone biopsy is the only method capable of demonstrating changes in bone microarchitecture, its use is restricted to the iliac crest. BTMs are an important means of obtaining information on changes in bone resorption and bone formation, but the findings reflect the integrated response across the whole skeleton. Radionuclide imaging studies give a unique method of studying bone turnover that is specific to the skeletal ROI chosen for study. Dynamic ^{18}F -PET imaging of bone is restricted by the 15-cm axial field of view of the scanner, but after completion of a dynamic scan to measure regional plasma clearance at a single site such as the lumbar spine, a series of spot views can be obtained to examine SUVs at any number of additional sites.

In the present study, dynamic PET scans of the lumbar spine showed a 24% increase in ^{18}F -plasma clearance after 6 months of treatment with teriparatide. Radionuclide tracers such as ^{18}F -bind to newly mineralizing bone, thus serving as markers of bone blood flow and osteoblastic activity.⁽¹⁷⁾ The mechanism of uptake in bone is the deposition of fluoride ions in newly forming hydroxyapatite crystals at sites of bone formation, and hence the component of bone turnover being measured by ^{18}F -imaging is osteoblastic activity. Equation 1 shows that the value of K_1 can change in response to a change in bone blood flow (K_1) or a change in the fraction of tracer entering the bone ECF compartment going to bone mineral ($k_3/[k_2 + k_3]$), or both. The results of the present study showed no change in K_1 but a 23% increase in $k_3/(k_2 + k_3)$, suggesting that the primary effect of

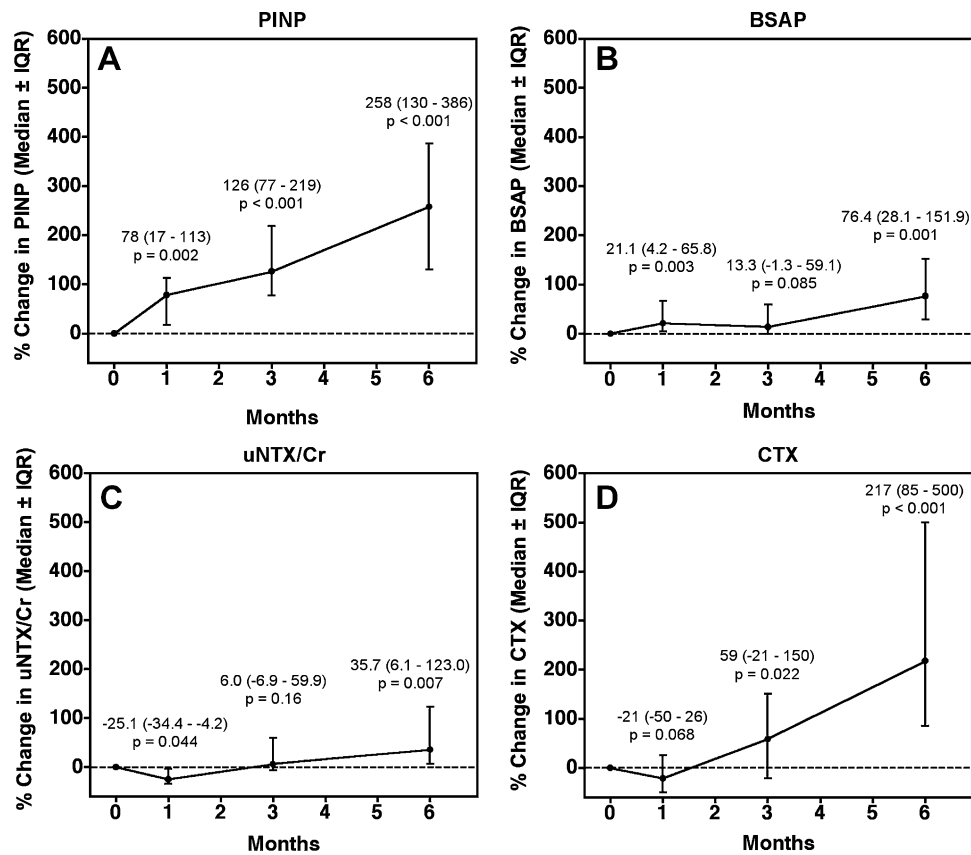


Fig. 3. Median percent changes from baseline of the bone turnover markers after 1, 3 and 6 months of teriparatide. Error bars show the interquartile range. *P*-values are calculated using the two-sided Wilcoxon signed rank test. (A) Serum procollagen propeptide of type 1 collagen (PINP); (B) serum bone-specific alkaline phosphatase (BSAP); (C) urinary cross linked N-telopeptide of type-1 collagen normalized to creatinine (uNTX/Cr); (D) serum cross-linked C-telopeptide of type 1 collagen (CTX).

teriparatide treatment was an increase in the density of sites for tracer deposition in the bone mineral compartment, consistent with increased osteoblastic activity. This interpretation of the results is supported by two studies that examined the relationship between K_i and bone histomorphometry and reported high correlations with histomorphometric indices of bone formation and mineral apposition rate but not with other indices.^(24,25)

In contrast to the findings presented here for teriparatide, Frost et al. reported an 18% decrease in K_i values at the lumbar spine in 18 postmenopausal women treated with risedronate for 6 months.⁽²¹⁾ As in the present study, bone blood flow was unchanged, and the decrease in K_i was explained by an 18% decrease in $k_3/(k_2 + k_3)$. In the only other study we are aware of that used ^{18}F -PET to examine the regional effects of an osteoporosis therapy, Uchida et al. reported a 14% decrease in SUVs at the spine and a 24% decrease at the femoral neck in 24 postmenopausal women treated with alendronate for 12 months for glucocorticoid-induced osteoporosis.⁽²⁷⁾

In the present study, although there was a highly significant change in ^{18}F -plasma clearance at the lumbar spine, SUVs at this site were almost unchanged. The 3% increase in SUVs after 6 months of treatment with teriparatide was explained by the 24% increase in spine plasma clearance being almost canceled by a 20% decrease in ^{18}F -plasma concentration. Unlike the response to treatment shown by plasma clearance measure-

ments, which solely reflect the physiological changes occurring at the chosen ROI, SUVs are a type of uptake measurement, and the changes observed are influenced by the fact there is only a finite amount of tracer available that has to be shared between a large number of competing sites, including bone, kidneys, soft tissue, and the vascular system. Therefore, the local changes in SUVs are affected by the competition for the available tracer across the entire body, including the rest of the skeleton.⁽³³⁾

If the skeletal effects of teriparatide led to the same percentage increase in regional plasma clearance values across the whole skeleton, one would expect the change in spine K_i to be partly explained by an increase in SUVs and partly by a decrease in ^{18}F -plasma concentration, with the latter reflecting the larger proportion of the injected dose being laid down in bone in response to treatment. A 24% increase in K_i values in the spine with no change in SUVs suggests that the skeletal effects of teriparatide must differ at different sites, with the small or absent change in SUVs at the spine explained by greater increases in K_i at other sites in the skeleton, which take up more of the injected dose, leaving less available for uptake in the spine.

Independent evidence that the skeletal effects of teriparatide treatment vary at different sites was reported by Moore et al., who found greater visual increases in uptake at the skull and lower extremities on whole-body $^{99\text{m}}\text{Tc}$ -MDP bone scans and four-times-larger increases in $^{99\text{m}}\text{Tc}$ -MDP plasma clearance at the

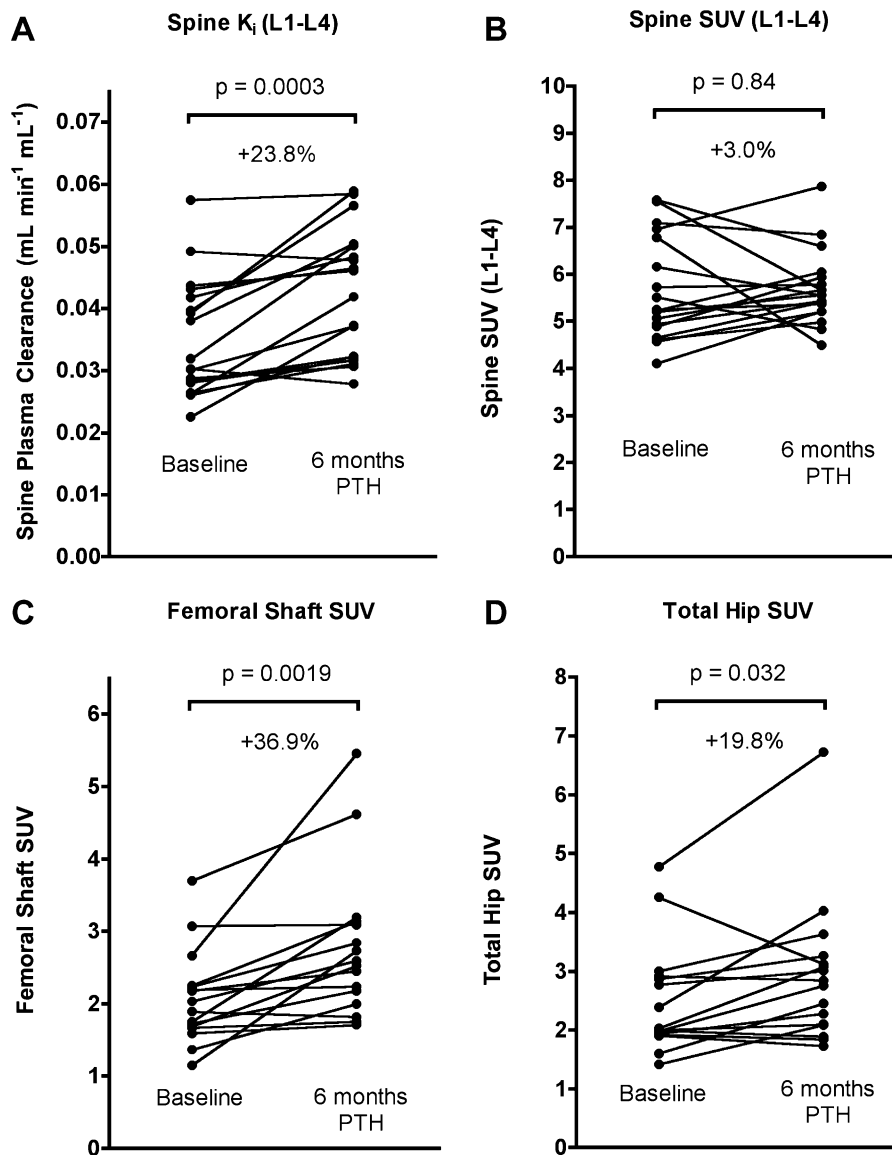


Fig. 4. Plots of the baseline to 6-month changes in individual subjects of: (A) Net ^{18}F -fluoride lumbar spine plasma clearance (K_i) measured using the Hawkins model; (B) Lumbar spine standardized uptake values (SUVs) (52–60 minutes); (C) Femoral shaft SUV (65–75 minutes); (D) Total hip SUV (65–75 minutes).

calvarium than at the spine.⁽³⁴⁾ The present study also found direct evidence for differences in the skeletal effects of teriparatide at different sites, with a 37% increase in SUVs at the femoral shaft compared with a 20% increase at the total hip site, and an 11% increase at the pelvis but only 3% for the spine. Unfortunately, it is not possible to infer the exact changes in K_i from those in SUVs, since the relationship depends on factors such as the relative contribution to SUVs of tracer in the bone ECF compartment, as well as any differences in the regional value of k_d , and these can only be investigated by performing dynamic scans. Assuming these factors are similar for different sites, the predicted increase in K_i values would be 34% for the pelvis, 44% for the total hip, and 65% for the femoral shaft, compared with the 24% increase found at the spine.

Perhaps the most interesting finding of the present study was the difference in SUV changes between the trabecular bone site

in the spine and the cortical site at the femoral shaft. Results for the total hip site and the pelvis were intermediate between the spine and femoral shaft and can be explained by the mix of cortical and trabecular bone at these two ROI. An anabolic effect of teriparatide on human cortical bone was previously reported from bone biopsy studies,^(13,14,16) although these were based on bone samples taken from the iliac crest and not all histology studies have shown such a pronounced effect on cortical bone.⁽¹⁵⁾

There is a striking disparity between the present findings and the results of bone densitometry studies of the effects of teriparatide treatment at the spine and proximal femur.^(5,35–38) DXA scan results from the present study are consistent with earlier findings from clinical trials that showed large increases in lumbar spine BMD with more modest changes at the hip.^(5,35,36) Results of total-body DXA scans, which are sensitive to

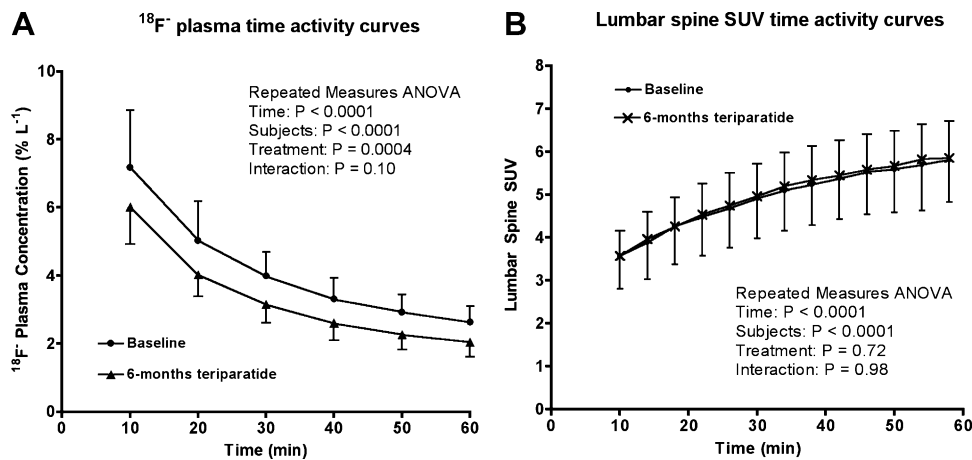


Fig. 5. (A) Plot of mean ^{18}F -fluoride venous plasma concentrations at 10, 20, 30, 40, 50, and 60 minutes after injection plotted as the percentage of injected dose per liter. ^{18}F activity has been corrected for radioactive decay. The two curves show the data at baseline and after 6 months of treatment with teriparatide. (B) Plot of mean lumbar spine standardized uptake values (SUVs) measured at 4-minute intervals (8–12; 12–16; 16–20; 20–24; 24–28; 28–32; 32–36; 36–40; 40–44; 44–48; 48–52; 52–56; 56–60 min). The two curves show the data at baseline and after 6 months of treatment with teriparatide. Curves were analyzed using a repeated-measures ANOVA.⁽³²⁾

the treatment effects on cortical bone across the whole skeleton, also showed only a small increase in total body bone mineral content.^(5,35) Studies using quantitative computed tomography (QCT) are a particularly sensitive means of comparing the effects of teriparatide treatment on BMD at trabecular and cortical bone sites in the spine and hip. The results show a large treatment effect on trabecular bone at the spine, a smaller effect on trabecular bone at the hip, and modest or absent effects on BMD in cortical bone, especially the hip.^(36–38) There have been fewer studies of the effect of teriparatide on cortical bone sites in long bones. Zanchetta et al. used peripheral QCT to study the nondominant distal radius and found increases in cortical bone mass and cross-sectional moment of inertia.⁽³⁹⁾ In contrast, a study of subjects from the Fracture Prevention Trial using DXA hip structure analysis (HSA) showed only modest improvements at the femoral neck and intertrochanteric sites, with no change at the femoral shaft.⁽⁴⁰⁾ The present results imply that that changes in bone density at different skeletal sites do not relate in any simple manner to the changes in K_i and suggest that large increases in bone formation rate may not necessarily translate into increases in bone density.

The principal limitation of this study is the lack of dynamic PET scan data at the hip to directly measure the effects of teriparatide treatment on bone plasma clearance at the femoral neck, total hip, and femoral shaft sites. Although it is a reasonable inference

from the SUV measurements that the changes in K_i in cortical bone at the hip will be greater than at the spine, this requires verification by dynamic PET scans of the hip. Another limitation is that the present study did not include a control group. Antifracture trials show that treatment with calcium and vitamin D alone has a mild antiresortive effect,^(2–4,6,7) and it is possible that this may have slightly blunted the anabolic effects of teriparatide reported in the present study.

In summary, we have used ^{18}F -PET imaging to examine the anabolic effects of teriparatide treatment on the rate of bone formation at both trabecular and cortical sites. After 6 months of treatment with teriparatide there was a 24% increase in ^{18}F -plasma clearance to bone mineral at the lumbar spine, with no significant changes in the other parameters of the three-compartment model except for the fraction of tracer going from the bone ECF compartment to bone mineral. In contrast to spine K_i values, SUVs, a measurement of bone uptake, increased by only 3%. This finding implies that the response to teriparatide varies between skeletal sites, with some sites showing considerably larger changes in plasma clearance compared with the spine. Measurements of SUVs in cortical bone in the femoral shaft showed a 37% increase at this site, which was statistically significantly greater than in the spine. Intermediate results were found for the pelvis and total hip sites. The SUV findings imply that treatment with teriparatide brings about larger percentage changes in bone formation in cortical bone

Table 3. Spearman Rank Correlation Coefficients Between Changes in K_i and Changes in Bone Turnover Markers After 6 Months of Teriparatide Therapy

	PINP	Bone BSAP	uNTX	sCTX
K_i	0.046 ($p = .87$)	0.124 ($p = .65$)	0.187 ($p = .52$)	0.256 ($p = .34$)
PINP	–	0.873* ($p < .0001$)	0.780* ($p = .0010$)	0.503* ($p = .040$)
Bone BSAP	–	–	0.718* ($p = .0026$)	0.271 ($p = .28$)
uNTX	–	–	–	0.443 ($p = .098$)

* $p < .05$ (two-tailed test)

than in trabecular bone and are at striking odds with the published findings from bone densitometry.

Disclosures

Drs. Frost and Fogelman received a research grant from Eli Lilly and Company as clinical trial investigators. Dr Eastell has received grant support and consultancy fees from Eli Lilly and Company. All other authors state that they have no conflicts of interest.

Acknowledgments

We thank Fatma Gossiel (Academic Unit of Bone Metabolism, University of Sheffield) for the measurements of the bone turnover markers. This study was supported by a grant from Eli Lilly.

References

1. Storm T, Thamsborg G, Steiniche T, et al. Effect of intermittent cyclical etidronate therapy on bone mass and fracture rate in women with postmenopausal osteoporosis. *N Engl J Med.* 1990;322:1265–1271.
2. Black DM, Cummings SR, Karpf DB, et al. Randomised trial of the effect of alendronate on risk of fracture in women with existing vertebral fractures. *Lancet.* 1996;348:1535–1541.
3. Ettinger B, Black DM, Mitlak BH, et al. Reduction of vertebral fracture risk in postmenopausal women with osteoporosis treated with raloxifene: results from a 3-year randomized clinical trial. *JAMA.* 1999;282:637–645.
4. Harris ST, Watts NB, Genant HK, et al. Effects of risedronate treatment on vertebral and non-vertebral fractures in women with postmenopausal osteoporosis. *JAMA.* 1999;282:1344–1352.
5. Neer RM, Arnaud CD, Zanchetta JR, et al. Effect of recombinant human parathyroid hormone (1-34) fragment on spine and non-spine fractures and bone mineral density in postmenopausal osteoporosis. *N Engl J Med.* 2001;344:1434–1441.
6. Chesnut CH, Skag A, Christiansen C, et al. Effects of oral ibandronate administered daily or intermittently on fracture risk in postmenopausal osteoporosis. *J Bone Miner Res.* 2004;19:1241–1249.
7. Black DM, Delmas PD, Eastell R, et al. Once-yearly zoledronic acid for treatment of postmenopausal osteoporosis. *N Engl J Med.* 2007;356:1809–1822.
8. Cummings SR, San Martin J, McClung MR, et al. Denosumab for prevention of fractures in postmenopausal women with osteoporosis. *N Engl J Med.* 2009;361:756–765.
9. Garnero P, Weichung JS, Gineyts E, et al. Comparison of new biochemical markers of bone turnover in late postmenopausal osteoporotic women in response to alendronate treatment. *J Clin Endocrinol Metab.* 1994;79:1693–1700.
10. Greenspan SL, Bone HG, Ettinger MD, et al. Effect of recombinant human parathyroid hormone (1-84) on vertebral fracture and bone mineral density in postmenopausal women with osteoporosis: a randomized trial. *Ann Intern Med.* 2007;146:326–339.
11. Glover SJ, Eastell R, McCloskey EV, et al. Rapid and robust response of biochemical markers of bone formation to teriparatide therapy. *Bone.* 2009;45:1053–1058.
12. McClung MR, San Martin J, Miller PD, et al. Opposite bone remodeling effects of teriparatide and alendronate in increasing bone mass. *Arch Intern Med.* 2005;165:1762–1768.
13. Dempster DW, Cosman F, Kurland ES, et al. Effects of daily treatment with parathyroid hormone on bone microarchitecture and turnover in patients with osteoporosis: a paired biopsy study. *J Bone Miner Res.* 2001;16:1846–1853.
14. Jiang Y, Zhao JJ, Mitlak BH, et al. Recombinant human parathyroid hormone (1-34) [teriparatide] improves both cortical and cancellous bone structure. *J Bone Miner Res.* 2003;18:1932–1941.
15. Arlot M, Meunier PJ, Boivin G, et al. Differential effects of teriparatide and alendronate on bone remodeling in postmenopausal women assessed by histomorphometric parameters. *J Bone Miner Res.* 2005;20:1244–1253.
16. Lindsay R, Zhou H, Cosman F, et al. Effects of a one-month treatment with PTH(1-34) on bone formation on cancellous, endocortical, and periosteal surfaces of the human ilium. *J Bone Miner Res.* 2007;22:495–502.
17. Blake GM, Park-Holohan S, Cook GJR, Fogelman I. Quantitative studies of bone with the use of ^{18}F -fluoride and $^{99\text{m}}\text{Tc}$ -methylene diphosphonate. *Semin Nucl Med.* 2001;31:28–49.
18. Hawkins RA, Choi Y, Huang S-C, et al. Evaluation of the skeletal kinetics of fluorine-18-fluoride ion with PET. *J Nucl Med.* 1992;33:633–642.
19. Schiepers C, Nuyts J, Bormans G, et al. Fluoride kinetics of the axial skeleton measured in vivo with fluorine-18-fluoride PET. *J Nucl Med.* 1997;38:1970–1976.
20. Cook GJ, Lodge MA, Marsden PK, et al. Non-invasive assessment of skeletal kinetics using fluorine-18 fluoride positron emission tomography: evaluation of image and population-derived arterial input functions. *Eur J Nucl Med.* 1999;26:1424–1429.
21. Frost ML, Cook GJR, Blake GM, et al. A prospective study of risedronate on regional bone metabolism and blood flow at the lumbar spine measured by ^{18}F -fluoride positron emission tomography. *J Bone Miner Res.* 2003;18:2215–2222.
22. Installe J, Nzeusseu A, Bol A, et al. ^{18}F -fluoride PET for monitoring therapeutic response in Paget's disease of bone. *J Nucl Med.* 2005;46:1650–1658.
23. Frost ML, Blake GM, Park-Holohan SJ, et al. Long-term precision of ^{18}F -fluoride PET skeletal kinetic studies in the assessment of bone metabolism. *J Nucl Med.* 2008;49:700–707.
24. Messa C, Goodman WG, Hoh CK, et al. Bone metabolic activity measured with positron emission tomography and ^{18}F -fluoride ion in renal osteodystrophy: correlation with bone histomorphometry. *J Clin Endo Metab.* 1993;77:949–955.
25. Piert M, Zittel TT, Becker GA, et al. Assessment of porcine bone metabolism by dynamic ^{18}F -fluoride PET: correlation with bone histomorphometry. *J Nucl Med.* 2001;42:1091–1100.
26. Brenner W, Bohuslavizki KH, Sieweke N, et al. Quantification of diphosphonate uptake based on conventional bone scanning. *Eur J Nucl Med.* 1997;24:1284–1290.
27. Uchida K, Nakajima H, Miyazaki T, et al. Effects of alendronate on bone metabolism in glucocorticoid-induced osteoporosis measured by ^{18}F -fluoride PET: a prospective study. *J Nucl Med.* 2009;50:1808–1814.
28. Kaufman JM, Orwoll E, Goemaere S, et al. Teriparatide effects on vertebral fractures and bone mineral density in men with osteoporosis: treatment and discontinuation of therapy. *Osteoporos Int.* 2005;16:510–516.
29. WHO. *Assessment of fracture risk and its application to screening for postmenopausal osteoporosis: technical report series 843.* Geneva: WHO, 1994.
30. Patel R, Blake GM, Rymer J, et al. Long-term precision of DXA scanning assessed over seven years in forty postmenopausal women. *Osteoporos Int.* 2000;11:68–75.
31. Looker AC, Wahner HW, Dunn WL, et al. Proximal femur bone mineral levels of US adults. *Osteoporos Int.* 1995;5:389–409.
32. Park E, Cho M, Ki C-S. Correct use of repeated measures analysis of variance. *Korean J Lab Med.* 2009;29:1–9.
33. Blake GM, Frost ML, Fogelman I. Quantitative radionuclide studies of bone. *J Nucl Med.* 2009;50:1747–1750.

34. Moore AE, Blake GM, Taylor KA, et al. Assessment of regional changes in skeletal metabolism following 3 and 18 months of teriparatide treatment. *J Bone Miner Res.* 2010;25:960–967.
35. Lindsay R, Nieves J, Formica C, et al. Randomised controlled study of effect of parathyroid hormone on vertebral-bone mass and fracture incidence among postmenopausal women on oestrogen with osteoporosis. *Lancet.* 1997;350:550–555.
36. Black DM, Greenspan SL, Ensrud KE, et al. The effects of parathyroid hormone and alendronate alone or in combination in postmenopausal osteoporosis. *N Engl J Med.* 2003;349:1207–1215.
37. Bauer DC, Garnero P, Bilezikian JP, et al. Short-term changes in bone turnover markers and bone mineral density response to parathyroid hormone in postmenopausal women with osteoporosis. *J Clin Endocrinol Metab.* 2006;91:1370–1375.
38. Cann CE, Roe EB, Sanchez SD, Arnaud CD. PTH effects in the femur: envelope specific responses by 3DQCT in postmenopausal women. *J Bone Miner Res.* 1999;14:S137 (abstract).
39. Zanchetta JR, Bogado CE, Ferretti JL, et al. Effects of teriparatide [recombinant human parathyroid hormone (1-34)] on cortical bone in postmenopausal women with osteoporosis. *J Bone Miner Res.* 2003;18:539–543.
40. Uusi-Rasi K, Semanick LM, Zanchetta JR, et al. Effects of teriparatide [rhPTH (1-34)] treatment on structural geometry of the proximal femur in elderly osteoporotic women. *Bone.* 2005;36:948–958.